STUDY ON THE MOVEMENT CHARACTERISTICS OF RAPESEED THRESHING MATERIALS BASED ON DEM SIMULATION AND HIGH-SPEED IMAGING
/
基于 DEM 和高速摄影技术的油菜籽脱粒物料迁移特性研究

Guangchao ZHAN*[1)], Wei LIU[2)], Peng ZHANG[1)]
[1)] School of Electromechanical and Intelligent Manufacturing, Huanggang Normal University, Huanggang 438000, Hubei, China
[2)] Jiangshan Heavy Industries Research Institute Co., Ltd., Norinco Group, Xiangyang Hubei 441005, China
Tel: +86-180-8650-1301; E-mail: guangchaozhan@hgnu.edu.cn
DOI: https://doi.org/10.35633/inmateh-76-107

Keywords: *rapeseed; threshing drum; DEM simulation; high-speed imaging; movement characteristics*

ABSTRACT
To investigate the movement characteristics and distribution patterns of materials inside the threshing drum during the rapeseed threshing process, a simplified DEM model was established using three typical particle types: seeds, pods, and stalks. A simulation system of the drum's internal environment was constructed, and combined with high-speed photography experiments to analyse the material distribution and dynamic movement trajectories. The results showed that materials primarily migrated in a helical pattern along the outer edge of the drum. Seeds and pods were mainly concentrated in collection box 2, accounting for 33.6% and 27.6% of the total, respectively. The material quantity gradually decreased from collection boxes 2 to 6, while 56.5% of the partially unbroken stalks were discharged from the straw outlet and collected in box 7. To verify the accuracy of the simulation, a test platform was built and high-speed photography experiments were conducted, showing that the actual material trajectories closely matched the simulation. Both simulation and experimental results indicated the highest material concentration in collection box 2, at 24.6% and 19.2%, respectively, and the lowest in box 6, at 5.1% and 6.8%. These findings provide theoretical support and technical guidance for optimizing drum structure, achieving precise threshing control, and advancing intelligent agricultural machinery design.

摘要
为研究油菜籽脱粒过程中脱粒滚筒内部物料的迁移特征和分布规律，建立了籽粒、果荚和茎秆三种典型颗粒简化的 DEM 模型。建立了脱粒滚筒内部环境模拟系统，并结合高速摄影实验对物料分布和动态迁移轨迹进行了分析。结果表明，物料主要沿滚筒外缘呈螺旋状迁移。种子和豆荚主要集中在 2 号收集箱，分别占总量的 33.6% 和 27.6%。从 2 号收集箱到 6 号收集箱，物料量逐渐减少，56.5% 的部分未破碎茎秆从秸秆出口排出，被收集到 7 号收集箱。为了验证模拟的准确性，我们搭建了一个测试平台，并进行了高速摄影实验，结果表明实际的物料轨迹与模拟非常吻合。模拟和实验结果都表明，2 号收集箱的物料浓度最高，分别为 24.6% 和 19.2%，6 号收集箱的物料浓度最低，分别为 5.1% 和 6.8%。这些发现为优化滚筒结构、实现精确脱粒控制和推进智能农机设计提供了理论支持和技术指导。

INTRODUCTION
As a critical stage in the mechanized harvesting of rapeseed, the performance of threshing directly affects key indicators such as seed loss rate, damage rate, and threshing efficiency *(Qing, 2021; Kuai, 2015; Pari, 2012)*. At present, mainstream rapeseed threshing devices both domestically and internationally predominantly adopt axial-flow or transverse-flow drum structures *(Yuan, 2024; Vlădut, 2023)*. Among them, axial-flow drums are widely applied in China's major rapeseed-producing areas due to their advantages in layered threshing and high efficiency *(Wan, 2018; Tang, 2024)*.

To enhance threshing performance, recent research efforts in China have focused on structural optimization of rapeseed threshing drums. Innovations include composite threshing devices, conical drum structures, variable-diameter drums *(Wang, 2023; Li, 2020; Chen, 2025)*, and differential-speed threshing mechanisms. These designs aim to develop a threshing unit with strong adaptability, low loss, and high versatility *(Wang, 2017; Xu, 2019; Wan, 2023)*.

[1] *Guangchao Zhan, Lecture, Ph.D; Wei Liu, Engineer, Ph.D; Peng Zhang, Lecture, Ph.D.*

However, most of the existing studies emphasize rotor or threshing component optimization and parameter regulation, while the impact of internal material movement characteristics on threshing performance remains largely underexplored. Given the significant variability in ripeness, moisture content, and plant morphology across different rapeseed fields *(Bruce, 2001; Ma, 2015; Liao, 2019)*, the mixture of seeds, pods, and stalks during the threshing process frequently leads to issues such as material clogging, accumulation, and repeated striking and over-crushing of stalks *(Mircea, 2020)*. These problems severely hinder threshing and separation efficiency during the combine harvesting process.

To overcome the limitations of traditional experimental methods in observing internal particle movement, DEM has been widely adopted in agricultural machinery simulation. *Wu et al. (2022)* developed a DEM-based rapeseed threshing model for parameter optimization. *Guan et al (2022)* proposed a flexible stalk model to improve simulation accuracy. *Fu et al (2021)* analysed the distribution characteristics of mixed materials in axial-flow drums, and other researchers investigated the mechanism of threshing loss, offering reference for simulation parameter settings *(Tang, 2024; Lee, 2009; Vlădut, 2022)*. Nonetheless, current research still lacks dynamic tracking of spatial movement, path variation, and residence behaviour of materials inside the drum. Furthermore, simulation result validation methods remain limited, which compromises the credibility and generalizability of the models.

High-speed photography, a non-contact and instantaneous visualization technique, has recently been applied to monitor agricultural operations and track particle motion. *Zhan et al (2022)* studied the dynamic response of rapeseed plants under vibration using high-speed imaging. Other researchers used high-speed cameras to evaluate the impact of different threshing elements on seed damage *(Ma, 2020; Lian, 2022)*. Some researchers combined image analysis to investigate the motion trajectories and threshing states of stalks and seeds, demonstrating the potential of high-speed photography in particle motion studies *(Zong, 2013; Zuo, 2014; Li, 2021)*. However, due to limitations such as restricted viewing angles, image occlusion, and high particle density, high-speed imaging alone is insufficient to fully reveal internal motion mechanisms.

In summary, although the research on rapeseed threshing devices has made notable progress, the internal movement mechanism of materials, particle movement paths, and residence distribution inside the drum remain under-investigated. Additionally, there is a lack of a high-confidence modelling and validation framework. Therefore, this study proposes a combined approach using DEM simulation and high-speed visual analysis. A simulation model of rapeseed threshing materials is developed to analyse their dynamic movement within the drum. Experimental validation is conducted through bench tests coupled with high-speed photography, aiming to reveal the material movement characteristics during the threshing process. This study provides theoretical support for structural optimization of the threshing drum and the design of intelligent agricultural machinery.

MATERIALS AND METHODS

Theoretical analysis

During the rapeseed threshing process, the axial movement of materials mainly relies on the spiral feeding head and the guiding spiral. The determination of the key parameter, screw angle, directly affects the efficiency of axial material movement. A force analysis showing how the spiral feeding head and guiding spiral act on the materials is presented in Figure 1.

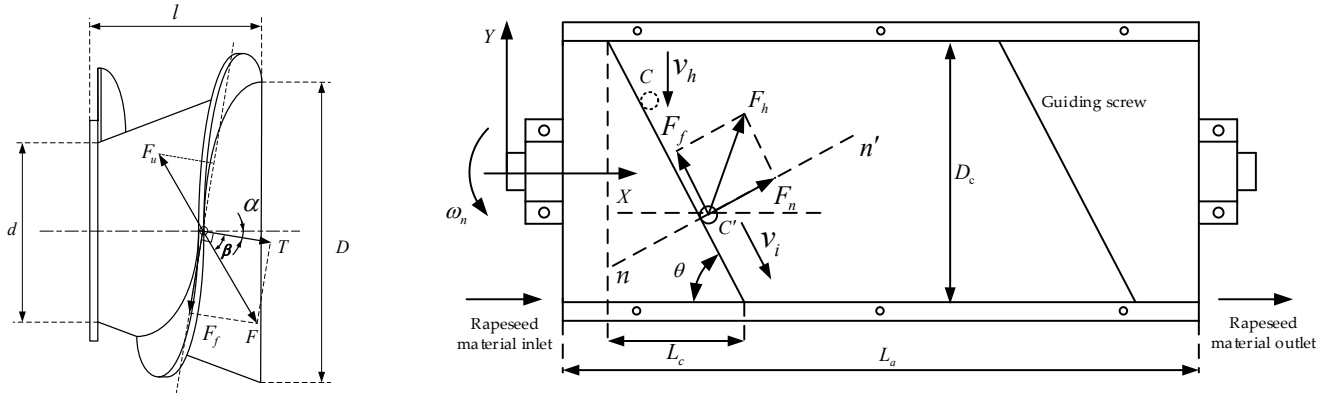

(a) Screw feed head of threshing drum *(b) Upper cover of rapeseed threshing drum*

Fig. 1 - Force analysis of guiding components in the rapeseed threshing drum

In Figure 1(*a*), T represents the normal thrust exerted by the helical blade on the rapeseed material, and its direction is perpendicular to the blade surface. When conveying the material, the helical blade generates a friction force F_f with the material, which lies in the blade surface and is perpendicular to the normal thrust T. The resultant force F is the combination of T and F_f. F_u is the resistance force acting on the material. The angle between the normal thrust T and the horizontal axis of the helical feed head is denoted as α, and the friction angle β between the rapeseed material and the helical blade is the angle between F and T. The angle α, corresponding to the helix angle, plays a critical role in feed performance. If the angle is too small, material feeding becomes slow and prone to clogging. Conversely, an excessively large angle can lead to unstable and pulsating feed flow, which is particularly unfavourable for lightweight crops such as rapeseed. Based on empirical data, the helix angle is typically within the range of 15° to 30°. In this design, the angle is set to 25°.

To facilitate observation of the actual threshing process of rapeseed, the upper cover is made transparent using organic glass. When the threshing device operates, the drum rotates at a high speed ω_n, and after the rapeseed material enters the threshing drum, it is subjected to high-speed striking and agitation by the threshing beaters mounted on the drum. Under this disturbance, the material moves in a circular path in the radial direction of the drum. Meanwhile, the guiding spiral conveys the material axially.

As shown in figure 1 (*b*), the rapeseed material, with mass m_c, contacts point C on the guiding spiral with an initial velocity v_h, then slides to point C', reaching a velocity v_i at that point. To enable the rapeseed material to slide and be conveyed along the axial direction of the drum, the angle between the guide spiral and the Y-axis must be less than the sliding friction angle of the rapeseed material, namely:

$$\begin{cases} 90° - \theta \le \varphi \\ \varphi \approx arctan\, \mu_c \end{cases} \quad (1)$$

In the equation, the symbol φ represents the sliding friction angle between the rapeseed material and the guiding spiral; while θ denotes the angle between the guiding spiral and the axial direction of the drum; and μ_c is the friction coefficient of the rapeseed material.

By simplifying Equation (1), the following is obtained:

$$\theta \ge 90° - arctan\, \mu_c \quad (2)$$

In the Yangtze River region of China, rapeseed is typically harvested with a relatively high moisture content. Under such conditions, the coefficient of friction of the material is taken as 0.58, thus, $\theta \ge 60°$. Furthermore, if angle θ is too large, the guiding efficiency of the spiral decreases, requiring additional guide spirals to achieve the desired conveying effect, therefore :

$$\begin{cases} tan\, \theta = \dfrac{D_c}{L_c} \\ L_c \ge \dfrac{L_a}{K_c} \end{cases} \quad (3)$$

where: D_c represents the width of the upper cover of the threshing drum, L_c denotes the lead of a single guiding spiral, L_a is the total length of the upper cover of the threshing drum, and K_c refers to the number of guiding spirals. Simplifying equation (3), the following is obtained:

$$\theta \le arctan \frac{K_c \cdot D_c}{L_a} \quad (4)$$

The width of the threshing drum upper cover D_c is directly determined by the threshing drum and is taken as 680 mm. The number of guiding spirals K_c is set to 8, and the length of the threshing drum upper cover L_a is 2.03 m. Therefore, $\theta \le 69.3°$. Considering all factors comprehensively, the helix angle θ of the guiding spiral is selected as 65°.

As shown in figure 2 (a), the grid-type concave screen generally consists of several components, including the side curved plates, transverse plates, and grate bars. Here, b_1 represents the spacing between adjacent transverse plates when they are evenly distributed, typically ranging from 30 to 40 mm; in this study, it is set to 40 mm. h_1 denotes the height by which the edge of a cross slat protrudes above the grate bars, which serves to assist in the threshing process. However, an excessive height may cause severe damage to the rapeseed stems. Therefore, h_1 is usually within the range of 5-15 mm, and is set to 10 mm in this design. a_1 indicates the spacing between grate bars. A smaller spacing may reduce the separation efficiency of the concave screen, while a larger spacing may lead to an increased loss of unthreshed pods and stalks falling through. Typically, the spacing ranges from 8 to 15 mm.

Considering that the material density at the front end of the threshing drum is higher than that at the rear end during operation, a two-section concave screen is adopted in this study: the front section has a spacing of 12 mm, and the rear section is set to 15 mm.

The wrap angle of the concave screen is illustrated in figure 2 (b). Since the wrap angle of the concave screen in rapeseed threshing devices is generally less than 180°, a wrap angle α_a of 150° is selected in accordance with the dimensions of the existing structure.

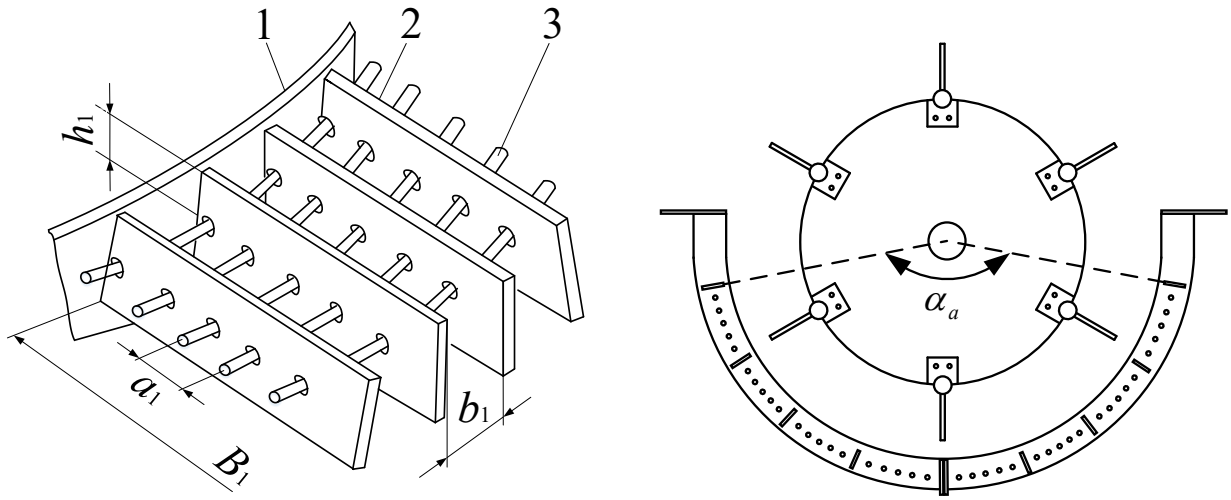

(a) Schematic diagram of the grid-type concave screen (b) Cross-sectional view of the concave screen

Fig. 2 - Schematic diagram of threshing elements

1. Side curved plate; 2. Transverse plate; 3. Grate bar

Material Modelling and Parameter Settings

Given the complex composition of materials involved in the actual threshing process, the simulation simplified the materials into three representative particle types: seeds, pods, and stalks. The seed model was simplified to a spherical particle with a diameter of 2 mm, based on the actual size of rapeseed grains. The stalks were modelled as cylindrical particles with a defined diameter, while the pods were simplified based on their actual morphological features. The simplified model is shown in the figure 3.

Seeds Pods Stalks

Fig. 3 - Simplified material model

The physical properties of each particle type were determined based on existing literature and experimental measurements. Detailed parameters are listed in Table 1 *(Shi, 2018)*.

Table 1

Parameter value of material simulation

Item	Poisson's Ratio	Density (kg·m^{-3})	Shear Modulus (MPa)
Seed	0.28	1060	11
Pods	0.30	1000	11
Stalks	0.30	809	47
Drum	0.30	7800	7000

Since all parts of the threshing drum were made of the same material, it was only necessary to define the contact parameters among the four types of materials: stalks, pods, seeds, and drum. The interaction parameters used in the contact simulation between these materials are listed in Table 2 *(Liao,2020)*. The main parameters include the coefficient of restitution between components, the static friction coefficient, and the rolling friction coefficient.

Table 2

Contact simulation parameters between materials

Item	Restitution Coefficient	Static Friction Coefficient	Rolling Friction Coefficient
Seed-Seed	0.41	0.54	0.01
Seed-Pod	0.30	0.47	0.01
Seed-Stalk	0.37	0.37	0.01
Seed-Drum	0.53	0.30	0.01
Pod-Pod	0.31	0.37	0.01
Pod-Stalk	0.35	0.32	0.01
Pod-Drum	0.34	0.43	0.01
Stalk-Stalk	0.41	0.29	0.01
Stalk-Drum	0.39	0.40	0.01

Based on the actual structural dimensions of the threshing drum, a simplified simulation model was constructed, including the drum, concave sieve, and guiding structures. Key parameters such as the drum diameter, length, and the arrangement of threshing beaters were set according to specifications commonly found in rapeseed threshing devices, with support for adjustable rotational speed to simulate different working conditions. In this study, the required materials were generated using a virtual factory approach, in which particles were introduced at a controlled rate over time. To better observe and compare the material distribution during the threshing process, the generation rate of particles was determined based on the actual feeding rate of rapeseed in field harvesting. Since the typical feeding rate of rapeseed is ≥2 kg/s and the harvesting speed is ≥0.9 m/s, the feeding rate was set to 20 rapeseed plants per second in the simulation. Statistical analysis of rapeseed plants shows that each plant contains approximately 254-478 pods, with each silique containing 12-33 seeds. A single plant has 8-12 branches, with branch lengths ranging from 46 to 87 mm. Considering these material characteristics and field operating parameters of rapeseed combine harvesters, the simulation was configured with a silique generation rate of 4,000 pods per second, a seed generation rate of 80,000 seeds per second, and a stalk generation rate of 100 stalks per second (with each stalk having a length of 200 mm).

Table 3

Statistical parameters of rape plant characters

Item	Numerical range	Average
Number of seeds (single pod)	12~33	21
Number of pods (single plant)	254~478	383
Number of branches (single plant)	8~12	10
Length of branch (mm)	46~87	64

High-Speed Photography Experiment

Fig. 4 - Main parameters of threshing test bench

1. Receiving plate; 2. Discharge port; 3. Concave screen; 4. Upper cover; 5. Threshing nail beater; 6. Guide screw; 7. Toothed rod; 8. Spiral feeding head; 9. Feeding port; 10. Drive motor; 11. Slide rail; 12. Electric push rod

The actual drum structure was consistent with the simulation model. The upper cover of the threshing drum was made transparent using organic glass to facilitate observation of the internal material movement by a high-speed camera. A receiving tray was placed below the drum to collect materials, and after threshing, manual screening was conducted to determine the distribution of seeds and other materials. The experimental setup is shown in figure 4.

By conducting high-speed photography observations of stalk breakage along the axial direction during the rapeseed threshing process, the motion trajectories and distribution of materials within the threshing unit can be intuitively understood. This method also enables the visualization of the interactions between rapeseed materials and key threshing components such as the rasp bars and guiding helices. Six collection boxes, each 200 mm in width, are arranged side by side beneath the drum sieve, with an additional box positioned at the end of the straw outlet. Figure 5 shows the experimental setup for axial observation during the rapeseed threshing process.

Fig. 5 - Test site of rape threshing process observed from axial direction

RESULTS

Simulation Results Analysis

To facilitate the observation of material movement trajectories, the simulation model was simplified by hiding the internal structure of the threshing drum rotor. After continuous feeding for 5 seconds, the materials inside the drum reached a relatively stable state. At this stage, randomly selected materials were observed to track their motion trajectories.

To better track individual particle movements, a single rapeseed stalk, pod, and seed were marked, and their motion trajectories were recorded. As shown in figure 6, the stalk, due to its larger size, could not easily pass through the concave sieve and exhibited a more complex trajectory before being discharged from the straw outlet at the end of the drum. In contrast, the smaller pods and seeds fell through the sieve more readily, showing simpler trajectories with distribution mainly concentrated in the front section of the sieve.

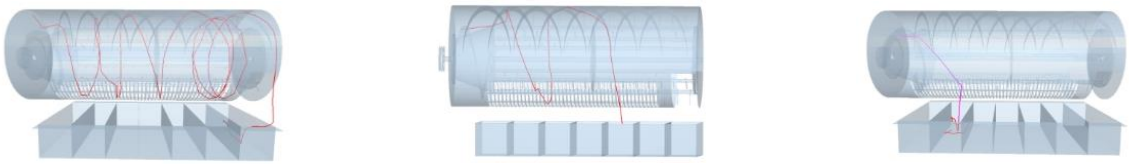

a. Trajectory of stalk b. Trajectory of pod c. Trajectory of seed

Fig. 6 - Motion trajectories of rapeseed materials inside the threshing drum

Keeping the material feeding rate constant, the simulation time was set to 5 seconds with a data saving interval of 0.01 seconds. After the simulation concluded, the process was paused at the 5-second mark. The DEM computational domain was divided into 8 × 1 × 3 regions along the axial, horizontal radial, and vertical directions of the threshing drum. The material distribution in each region was statistically analysed.

To investigate the distribution of stalks discharged from the drum, only the stalk distribution in the receiving box beneath the concave screen was considered. To reduce random errors, each simulation scenario was repeated three times, and the average values were taken. Figure 7 shows the material distribution diagram. In the figure, magenta particles represent rapeseed grains, green particles represent pods, and yellow particles represent stalks.

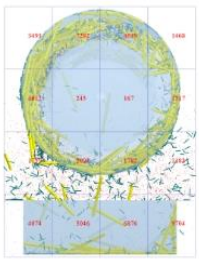

a. Radial distribution of seeds

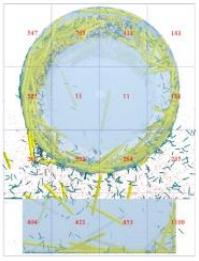

b. Radial distribution of pods

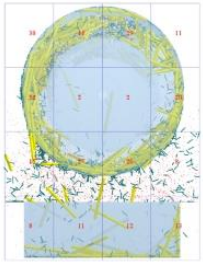

c. Radial distribution of stalks

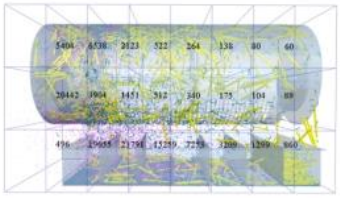

d. Axial distribution of seeds

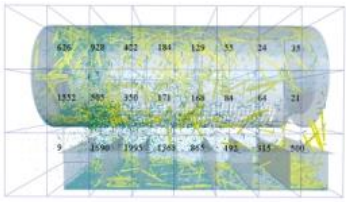

e. Axial distribution of pods

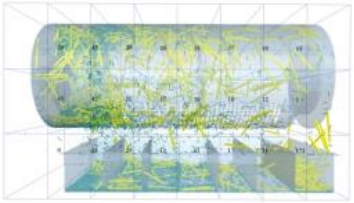

f. Axial distribution of stalks

Fig. 7 - Distribution of rapeseed materials in the threshing drum

Figure 7 presents the simulated material distribution within the threshing drum. The simulation results indicate that the radial distribution of materials is primarily concentrated near the outer periphery of the drum, with fewer materials located near the drum centre. Axially, the distribution of seeds and pods shows a clear decreasing trend from the front to the rear part of the drum.

Due to their larger size and frequent contact with the concave screen and threshing components inside the drum, the stalks exhibit the longest residence time and are mainly discharged from the straw outlet at the rear part of the drum. The pods rank second in residence time, with materials primarily distributed in the front half of the drum. The rapeseed grains, being the smallest, are the easiest to be discharged and have the shortest residence time inside the drum. These differences are directly related to threshing efficiency and separation performance.

High-Speed Photography Experimental Results

High-speed photography was used to observe and analyse the rapeseed threshing process. Figure 8 shows the axial movement and distribution of materials within the threshing drum. The high-speed photography experiments revealed that during the threshing process, materials were mainly distributed along the outer region of the drum. Under the combined action of threshing beaters and rods, the rapeseed materials migrated along the periphery of the threshing drum. The results of this experiment are in general agreement with the simulation.

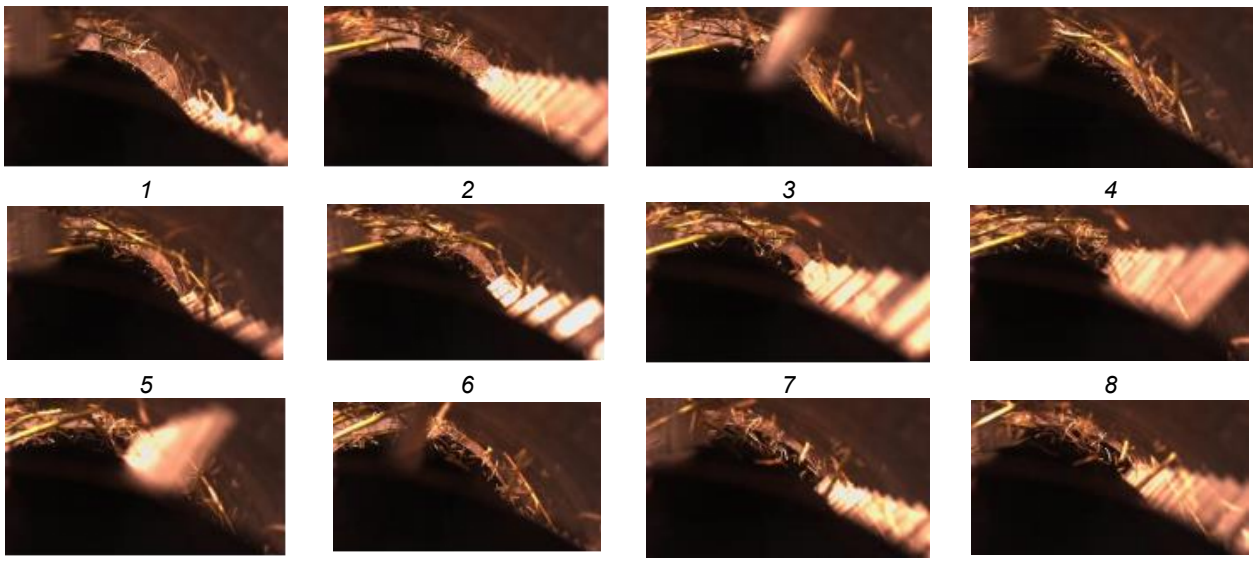

Fig. 8 - High-speed photography of material movement as rapeseed separates from the threshing drum

The distribution of materials in the collection bins after separation is shown in figure 9. Figure 9(*a*) shows the distribution of seeds, pods and stalks during the simulation process. To better replicate the real feeding process from the conveyor to the threshing drum, a horizontal initial velocity was assigned to the materials in the simulation. This velocity caused a portion of the materials to travel further before settling, resulting in a smaller quantity in collection box 1 and a greater accumulation in collection box 2. Seeds and pods were concentrated in collection box 2 with 33.6 % and 27.6%, respectively. From collection box 2 to box 6, the material amount shows a decreasing trend, and 56.5% of the partially unbroken stalks are discharged from the straw outlet of the threshing drum and fall into collection box 7, which contains the largest mass of material.

To estimate the mass of seeds, pods, and stalks in the simulation, the physical materials were scaled according to the dimensions used in the simulation model. Given that the thousand-grain weight of rapeseed is approximately 3.5 g, the mass of a single seed is about 0.0035 g. A single pod weighs approximately 0.5 g, and a mature 200 mm-long rapeseed stalk weighs about 5 g. Based on the material counts in each collection box, the corresponding mass distribution of different materials in the simulation was calculated. This simulated mass distribution was then compared with the results obtained from the actual threshing experiments.

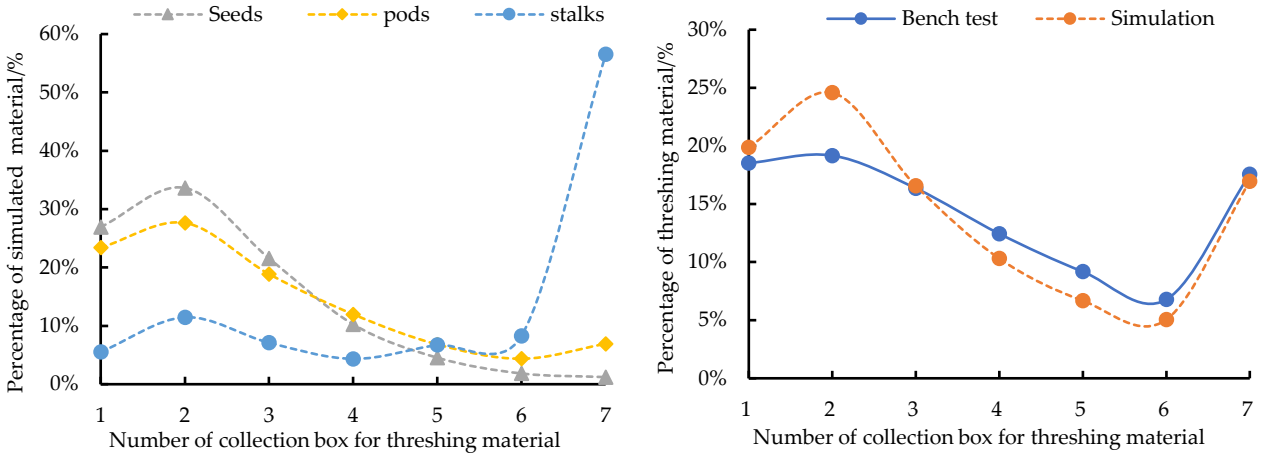

(*a*) Simulation of material distribution (*b*) Comparison of simulated and experimental

Fig. 9 - Threshing material distribution of collection boxes

Test results are shown in figure 9(b). The increase in material quantity from collection box 1 to box 2 is mainly because the materials are relatively intact upon entering the threshing drum; at this stage, pods and stalks have not yet fully separated, so the materials are less likely to fall into the bins. From Collection box 2 to 6, both the simulation and the bench-scale threshing experiment exhibit a gradual decrease in material quantity. The material distribution from both simulation and experiment was highest in collection box 2, accounting for 24.6% and 19.2%, respectively, while the lowest mass was observed in collection box 6, with 5.1% and 6.8%, respectively.

CONCLUSIONS

Based on DEM simulation and high-speed imaging visualization experiments, this study systematically investigated the movement characteristics and motion patterns of materials inside the rapeseed threshing drum. The results show that materials are mainly distributed around the beater bars near the drum periphery, with movement trajectories following a spiral motion along the drum's outer edge. The spiral direction is generally consistent with the guiding helix on the drum cover.

Significant differences in motion states were observed among different particle types within the drum. Stalks, due to their large size and frequent contact with the internal drum structures, exhibit the longest residence time; pods rank second; and seeds, being small and light, have the shortest residence time. The high-speed photography experiments validated the simulation model's accuracy and reliability regarding particle trajectories, velocity variation trends, and residence time distribution, ensuring the credibility of the simulation results. The distribution of rapeseed seeds and pods beneath the concave sieve exhibited a pattern of initial increase followed by a decrease, while the distribution of rapeseed stalks was relatively uniform.

However, there was a noticeable rise in stalk material near the discharge outlet, with 57% of the stalks exiting through this opening. A comparison between the bench test and simulation results revealed a consistent distribution trend, thereby confirming the reliability of the findings.

This study proposes a “simulation + visualization validation” methodological framework, providing new insights into the movement mechanisms of materials inside rapeseed threshing drums. The findings lay a technical foundation for developing efficient and low-loss intelligent threshing equipment. Future work could integrate intelligent sensing and control technologies to achieve real-time monitoring and adaptive regulation of the threshing process, promoting the intelligent and efficient development of rapeseed harvesting machinery.

ACKNOWLEDGEMENT

The authors gratefully acknowledge the support of the affiliated institution and the technical assistance provided during the research. Appreciation is also extended to the research group members for their valuable discussions. This project was funded by the Young Faculty Career Elevation Project (204202315604), and the University Distinguished Doctoral Research Program (2042023014).

REFERENCES

[1] Bruce, D., Hobson, R., Morgan, C., & Child, R. (2001). Threshability of shatter-resistant seed pods in oilseed rape. *Journal of Agricultural Engineering Research*, 80(4). 343–350. https://doi.org/10.1006/jaer.2001.0748

[2] Chen, L., Zhang, L., Li, L., & Zhang, L. (2025). Design and experiment of a low-damage threshing drum for corn with stepless taper adjustment. *Agriculture*, 15(1), 4. https://doi.org/10.3390/agriculture15010004

[3] Fu, J., Xie, G., Ji, C., Wang, W., Zhou, Y., Zhang, G., Zha, X., Abdeen, M. (2021). Study on the distribution pattern of threshed mixture by drum-shape bar-tooth longitudinal axial flow threshing and separating device. *Agriculture*, 11. https://doi.org/10.3390/agriculture11080756

[4] Guan, Z., Mu, S., Li, H., Jiang, T., Zhang, M., & Wu, C. (2022). Flexible DEM model development and parameter calibration for rape stem. *Applied Sciences*, 12(17). https://doi.org/10.3390/app12178394

[5] Kuai, J., Sun, Y., Zuo, Q., Huang, H., Liao, Q., Wu, C., Lu, J., Wu, J., & Zhou, G. (2015). The yield of mechanically harvested rapeseed (*Brassica napus L.*) can be increased by optimum plant density and row spacing. *Scientific Reports*, 5, 18835. https://doi.org/10.1038/srep18835

[6] Lee, C., Choi, Y., Jun, H., Lee, S., Moon, S., & Kim, S. (2009). Development of a rapeseed reaping equipment attachable to a conventional combine (III) – Analysis of principal factor for loss reduction of rapeseed mechanical harvesting. *Journal of Biosystems Engineering*, 34(2), 114–119. https://doi.org/10.5307/JBE.2009.34.2.114

[7] Li, X., Du, Y., Guo, J., & Mao, E. (2020). Design, simulation, and test of a new threshing cylinder for high moisture content corn. *Applied Sciences*, 10(14), 4925. https://doi.org/10.3390/app10144925

[8] Li, X., Wang, W., Zhao, G., Sun, C., Hu, P., & Ji, J. (2021). Design and experiment of longitudinal axial flow double flexible rolling and kneading threshing device for millet. *Transactions of the Chinese Society of Agricultural Machinery*, 52(7), 113–123. https://doi.org/10.6041/j.issn.1000-1298.2021.07.011

[9] Lian, G. D., Wei, X. X., Ma, L. N., Zhou, G. H., & Zong, W. Y. (2022). Design and experiments of the axial-flow spiral-drum threshing device for the edible sunflower. *Transactions of the Chinese Society of Agricultural Engineering*, 38, 42–51. DOI: 10.11975/j.issn.1002-6819.2022.17.005

[10] Liao, Q., Xu, Y., Yuan, J., Wan, X., & Jiang, Y. (2019). Design and experiment on combined cutting and throwing longitudinal axial flow threshing and separating device of rape combine harvester. *Transactions of the Chinese Society of Agricultural Machinery*, 50(7): 140-150. https://doi.org/10.6041/j.issn.1000-1298.2019.07.001

[11] Liao, Y., Liao, Q., Zhou, Y., Wang, Z., Jiang, Y., & Liang, F. (2020). Parameters calibration of discrete element model of fodder rape crop harvest in bolting stage. *Transactions of the Chinese Society of Agricultural Machinery*, 51(06):73-82. https://doi.org/10.6041/j.issn.1000-1298.2020.06.008

[12] Ma, Z., Han, M., Li, Y., Yu, S., & Chandio, A. (2020). Comparing kernel damage of different threshing components using high-speed cameras. *International Journal of Agricultural and Biological Engineering*, 06. 013. https://doi.org/10.25165/j.ijabe.20201306.5395

[13] Ma, Z., Li, Y., & Xu, L. (2015). Experimental study of reciprocating friction between rape stalk and bionic non-smooth surface units. *Applied Bionics and Biomechanics*, 627960. https://doi.org/10.1155/2015/627960

[14] Mircea, C., Nenciu, F., Vlăduț, V., Voicu, G., Gageanu, I., & Cujbescu, D. (2020). Increasing the performance of cylindrical separators for cereal cleaning by using an inner helical coil. *INMATEH – Agricultural Engineering*, 62(3), 249-258. https://doi.org/10.35633/inmateh-62-26.

[15] Pari, L., Assirelli, A., Suardi, A., Civitarese, V., Giudice, A., Costa, C., & Santangelo, E. (2012). The harvest of oilseed rape (Brassica napus L.): The effective yield losses at on-farm scale in the Italian area. *Biomass Bioenergy*, 46: 453-458. https://doi.org/10.1016/j.biombioe.2012.07.014

[16] Qing, Y., Li, Y., Xu, L., & Ma, Z. (2021). Screen Oilseed Rape (Brassica napus) Suitable for Low-Loss Mechanized Harvesting. *Agriculture,* 11(6), 504; https://doi.org/10.3390/agriculture11060504

[17] Shi, X., Wu, C., Li, H.; Qi, X., Yuan, J., Mei, Z., & Hu, T. (2018). Measurement and analysis of physical mechanical properties and aerodynamic characteristics of harvesting extractions from two rape varieties. *Jiangxi Agricultural Sciences*, 30(6). https://doi.org/10.19386/j.cnki.jxnyxb.2018.06.22

[18] Tang, Q., Jiang, L., Yu, W., Wu, J., & Wang, G. (2024). Design and experiment of high moisture corn threshing device with low damage. *INMATEH – Agricultural Engineering*, 74(3), 172-183. https://doi.org/10.35633/inmateh-74-15

[19] Vlădut, N., Biris, S., Cârdei, P., Găgeanu, I., Cujbescu, D., Ungureanu, N., Popa, L., Perişoară, L., Matei, G., & Teliban, G. (2022). Contributions to the mathematical modeling of the threshing and separation process in an axial flow combine. *Agriculture*, 12(10), 1520. https://doi.org/10.3390/agriculture12101520

[20] Vlădut, N., Ungureanu, N., Biris, S., Voicea, I., Nenciu, F., Găgeanu, I., Cujbescu, D., Popa, L., Boruz, S., Matei, G., Ekielski, A., & Teliban, G. (2023). Research on the identification of some optimal threshing and separation regimes in the axial flow apparatus. *Agriculture*, 13(4), 838. https://doi.org/10.3390/agriculture13040838

[21] Wan, X., Shu, C., Xu, Y., Y, J., Li, H., & Liao, Q. (2018). Design and experiment on cylinder sieve with different rotational speed in cleaning system for rape combine harvesters. *Transactions of the Chinese Society of Agricultural Engineering*, 34(14), 27–35. https://doi.org/10.11975/j.issn.1002-6819.2018.14.004

[22] Wan, X., Yuan, J., Yang, J., Liao, Y., & Liao, Q. (2023). Effects of working parameters on the performance of cyclone separator for rapeseed combine harvester based on CFD. *International Journal of Agricultural and Biological Engineering*, 16(1), 128–135. https://doi.org/10.25165/j.ijabe.20231601.7253

[23] Wang, F., Liu, Y., Li, Y., & Ji, K. (2023). Research and experiment on variable-diameter threshing drum with movable radial plates for combine harvester. *Agriculture*, 13(8), 1487. https://doi.org/10.3390/agriculture13081487

[24] Wang, G., Guan, Z., Mu, S., Tang, Q., & Wu, C. (2017). Optimization of operating parameter and structure for seed thresher device for rape combine harvester. *Transactions of the Chinese Society of Agricultural Engineering*, 33(24):52-57. https://doi.org/10.11975/j.issn.1002-6819.2017.24.008

[25] Wu, J., Tang, Q., Mu, S., Jiang, L., & Hu, Z. (2022). Test and optimization of oilseed rape (*Brassica napus L.*) threshing device based on DEM. *Agriculture*, 12(10), 1580. https://doi.org/10.3390/agriculture12101580

[26] Xu, L., Wei, C., Liang, Z., & Li, Y. (2019). Development of rapeseed cleaning loss monitoring system and experiments in a combine harvester. *Biosystems Engineering*, 178, 118–130. https://doi.org/10.1016/j.biosystemseng.2018.11.001

[27] Yuan, J, Liao, Q., Wan, X., Yang, J., & Shu, C. (2024). Parameter matching and experiment of the combined cyclone separation and cylinder sieve cleaning system for rape combine harvester. *International Journal of Agricultural & Biological Engineering*, 17(1), 128–136. https://doi.org/10.25165/j.ijabe.20241701.7739

[28] Zhan, G., Ma, L., Zong, W., Liu, W., Deng, D., & Lian, G. (2022). Study on the vibration characteristics of rape plants based on high-speed photography and image recognition. *Agriculture*, 12(5),727. https://doi.org/10.3390/agriculture12050727

[29] Zong, W., Liao, Q., Huang, P., Li, H., & Chen, L. (2013). Design of combined rape threshing device and analysis of rape cane movement trail. *Transactions of the Chinese Society of Agricultural Machinery*, 44:41-46. https://doi.org/10.6041/j.issn.1000-1298.2013. S2.009

[30] Zuo, Q., Huang, H., Cao, S., Yang, S., Liao, Q., Leng, S., Wu, J., & Zhou, G. (2014). Effects of harvesting date on yield loss percentage of mechanical harvesting and seed quality in rapeseed. *Acta Agronomica Sinica*, 40(04): 650-656. https://doi.org/10.3724/SP.J.1006.2014.00650